Steel and Composite Structures, *Vol. 35, No. 2 (2020) 171-186*
DOI: https://doi.org/10.12989/scs.2020.35.2.171

Burst capacity of pipe under corrosion defects and repaired with thermosetting liner

Ali Akram[1a], Zahiraniza Mustaffa*[1] and Thar M. Badri Albarody[2b]

[1]Department of Civil and Environmental Engineering, Universiti Teknologi PETRONAS, 32610, Seri Iskandar, Perak, Malaysia
[2]Department of Mechanical Engineering, Universiti Teknologi PETRONAS, 32610, Seri Iskandar, Perak, Malaysia

(*Received December 4, 2018, Revised December 10, 2019, Accepted April 10, 2020*)

Abstract. This paper aims at providing insights on the use of thermosetting liner for the repair of offshore pipelines exposed to corrosion and leakage. The work which covers both experimental and numerical approaches were aspired due to the high cost of repair for pipelines, limitations of thermoplastic material and limited study of reinforced thermosetting liner. The experiment involves a destruction test called the burst test, carried out on an API 5L X42 carbon steel pipe under four case studies, namely (i) intact pipe, (ii) pipe with corrosion defect, (iii) pipe with corrosion defect and repaired with thermosetting liner and (iv) pipe with leakage and repaired with thermosetting liner. The numerical simulation was developed to first validate the experimental results and later to optimize the design of the thermosetting liner in terms of the number of layers required to restore the original strength of the pipe. The burst test shows an improvement in 23% of the burst capacity for the pipe with corrosion defects, after being repaired with a three-layer thermosetting liner. The parametric studies conducted showed that with an addition of thermosetting layers, the burst capacity improves by an average of 1.85 MPa. In conclusions, the improvement in strength can be further increased with increasing thickness of the thermosetting liner. The thermosetting liner was also determined to fail first inside the host pipe.

Keywords: pipeline; corrosion; leakage; burst capacity; repair; thermosetting liner

1. Introduction

The integrity of pipelines has always been the highest priority for pipeline operators especially for ageing pipelines. Pipelines are susceptible to failure due to several source of damages where external interference and corrosion (Palmer and King 2004, Popineau *et al*. 2012, Sulaiman and Tan 2014) are the highest contributors as shown in Fig. 1.

The core issue of pipeline repairs is the high cost incurred, often in the range of millions of dollars (Mohammadi 2011) especially when involving pipeline replacement. A comparison made between an effort of rehabilitation of an old pipe and installation of a new pipe was reported earlier, for instance as shown in Fig. 2. The cost of installing a new pipe was found to be in the magnitude of three times higher than rehabilitation.

Therefore, various repair methods were developed with the aim of minimizing installation costs while maintaining efficiency. In this paper, the repair method considered is the use of reinforced liners, namely, reinforced thermoplastic pipes (RTP) for repair and rehabilitation.

The concept of repair is, for severe damages, instead of replacing the pipeline, an RTP is inserted inside the damaged pipe strengthening it from the inside. Furthermore, through this method, it was found that the installation cost could be reduced as much as 67% as shown in Fig. 3.

However, RTP is generally made from thermoplastic resin reinforced with synthetic fibers. Thus, the majority of RTP can rarely withstand high temperatures. (Anderson *et al.* 2012) specified that HDPE, a commonly used polymer for RTP, can generally withstand temperatures between 73°C to 90°C. (Anderson *et al.* 2012) further reported that the operating temperature of typical oil or gas pipelines is in the range of 1°C to 71°C. However, some oil fields can reach temperatures higher than 160°C (Hopkins 2005) thus making RTP unsuitable to be used.

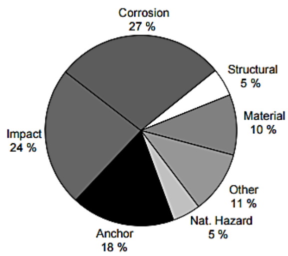

(a) The North Sea

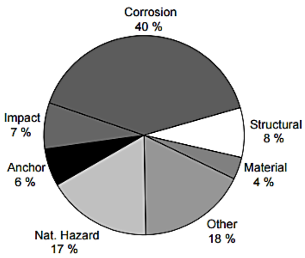

(b) The Gulf of Mexico

Fig. 1 Pipeline failures in the North Sea and the Gulf of Mexico (DNV-RP-F116, 2009)

*Corresponding author, Associate Professor
E-mail: zahiraniza@utp.edu.my
[a]MS.c
[b]Ph.D. Senior Lecturer

http://www.techno-press.org/?journal=scs&subpage=8
ISSN: 1229-9367 (Print), 1598-6233 (Online)

REHAB VS. NEW 36-IN MAIN OIL LINE

Cost element	Rehabilitate old main oil lines	Install new 36-in. main oil line
	Costs, $ million	
Rehabilitation costs	22	3
Intelligent pigging	2	1
New pipeline costs	-	75
Total:	**$24**	**$79**

Fig. 2 Sample of cost comparison between rehabilitation of old pipeline vs. installation of new pipeline (Morsi *et al.* 1997)

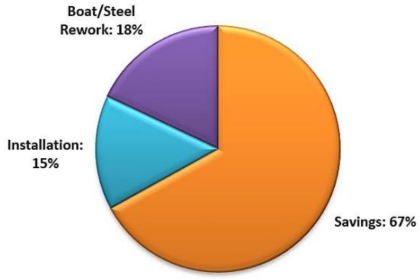

Fig. 3 Cost savings when using IFL (Morsi, Bayoumi and Robson 1997)

On the other hand, thermosetting, another type of polymer, have a stronger molecular structure than thermoplastics and thus have better mechanical properties (Kaw 1997). (Hancox 1991) reported that epoxy, a commonly used thermoset for high strength applications, is capable of experiencing temperature up to 180ºC depending on the post curing, reinforcement, grade, applied load, and environment. Furthermore, composites, specifically thermosets, have been studied before as a successful repair method for damaged structures. For example, Chen and Das (2009) studied the effect of strengthening corroded steel beam using carbon fiber reinforced polymer (CFRP). Similarly, Keykha (2017) studied the use of CFRP for corroded steel columns while Setvati and Mustaffa (2018) employed CFRP for rehabilitation of notched circular hollow sectional steel beam. Yang *et al*. (2017) investigated the design and mechanical performance of a concrete deck combined with glass fiber reinforced polymer (GFRP).

Therefore, a new RTP was developed by replacing the existing thermoplastic polymer with thermoset. The usage of thermosetting material in reinforced liner is an appealing notion as it will allow the reinforced liner to be deployed in high temperature and high-pressure conditions (HPHT) for rehabilitation purposes.

However, the implementation of thermosetting material in reinforced liners for rehabilitation of offshore pipeline is yet to be investigated, thus the need for further study involving physical experiments and numerical analysis to determine its performance. In this paper, the implementation of thermosetting material in reinforced liners is termed as a thermosetting liner.

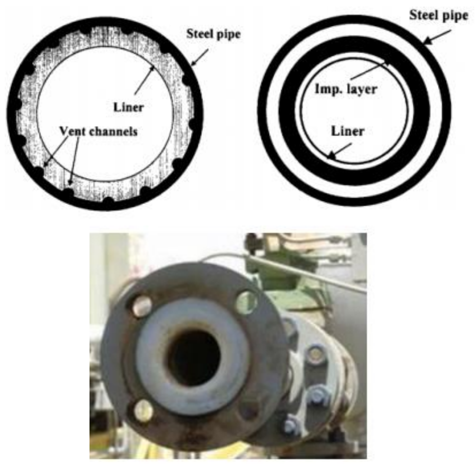

Fig. 4 Engineered liners (Frost *et al*. 2000, Mehdi and Al-dossary 2013)

2. Literature reviews

The concept of inserting a reinforced liner inside a damaged pipe not only offers additional strength, but also provides a corrosion resistant barrier on the inner surface of the pipe. However, corrosion resistant barriers have been utilized in several areas such as in offshore flexible pipelines and rigid pipelines in the form of a thermoplastic liner. The thermoplastic liners are usually made of HDPE but faces permeability issues (4 Subsea 2013, Do *et al.* 2013, Muren 2007, Obrien *et al.* 2011, Simonsen *et al.* 2012). Therefore, some liners are engineered to overcome permeability by introducing vent channels or adding additional layers as shown in Fig. 4. These liners, however, are not made to resist operating loads such as the internal pressure and thus could not be used for rehabilitation purposes.

Thus, numerous studies were conducted to investigate the suitability of reinforced liner as a rehabilitation method. Rehabilitation liners are seen more for onshore applications and only a handful for offshore pipelines. Table 1 summarizes recent studies conducted with regards to the rehabilitation liners for pipelines.

It can be seen that numerous researches have been conducted for reinforced liners as a rehabilitation method for pipelines. However, the majority of these studies focused more on onshore pipelines, specifically for buried pipelines where soil movements and compression loads are of great concern. For example, Abel (2015 a, b) has shown the effects of liner thickness and initial deflection towards the change in the load bearing capacity of the pipe. Nienartowicz (2015) also studied the load bearing capacity of a pipe inserted with a glass reinforced plastic liner with respect to mating, friction, and grout quality. On the other hand, Farhidzadeh *et al.* (2014) studied the effect of earthquake motion towards pipeline rehabilitated with a thermosetting liner through CIPP.

Limited studies have been conducted on reinforced liners for the rehabilitations of offshore pipelines, specifically using thermosetting reinforced liner. Reinforced

Table 1 Rehabilitation liners for damaged pipelines

Author	Rehabilitation liner	Resin	Reinforcement	Scope
(Abel 2015a, b)	Trolining liner	HDPE	V shaped embedment stud	Deflection, ring stiffness, load bearing capacities and rupture forces.
(Nienartowicz 2012, 2015)	GRP liner	Polyester	Glass fiber	Effect of mating, friction and quality of grout towards operating conditions and load capacity.
(Barsoum *et al.* 2016)	Kevlar Reinforced Liner	HDPE	Kevlar	Finite element analysis for installation process.
(Wright *et al.* 2014)	Reinforced Ther-moplastic Pipe	Polyphenyline Sulfide (PPS)	Aramid fiber	Material selection and installation process.
(Walters 2015)	Infield liner (IFL)	PVDF	Aramid fiber	Review on qualification and installation process of the IFL.
(Farhidzadeh *et al.* 2014)	Insituform IMain Liner	Thermoset	Fiber sleeve	Post-earthquake evaluation using CIPP.
(Carpenter 2016)	Glass reinforced vinyl ester	Vinyl Ester	Glass fiber	Material characterization.

thermoplastic liners, also known as RTP, has been studied for offshore pipelines in terms of qualification, installation, and application, as demonstrated by Wright *et al.* (2014) and Walters (2015). On the other hand, reinforced thermosetting pipes are mostly investigated as stand-alone pipes where some were focused on the material characterization as reported by Carpenter (2016).

Therefore, due to the limitations of thermoplastics in addition to limited studies conducted for thermosetting liners as a rehabilitation method for offshore pipelines, there is a need to conduct experimental testing complemented with numerical analysis to investigate the suitability of the thermosetting liners. Hence, the focus of this paper is to investigate the structural response of a pipe under corrosion defect and repaired with thermosetting liner through experimental tests and numerical analysis. A series of burst tests was conducted where the loading applied was only the internal pressure. The methodology for the experimental tests and numerical analysis will be presented in the next section.

3. Methodology

The method of investigation was divided into the physical experiment and numerical analysis. The aim was to develop a numerical model based on experimental results which could be used to conduct parametric studies, with thickness of the thermosetting liner as the changing variable. The flow of study is shown in Fig. 5.

3.1 Physical experiment

The physical experiment was aimed at obtaining data for developing the numerical model. The experiment involved a thermosetting liner made from glass epoxy prepregs insertedin an API 5L X42 carbon steel pipe with a single corrosion defect on the internal surface. The material properties of thesteel pipe were provided sufficiently by the manufacturer inthe form of a mill certificate which includes the maximum tensile strength, yield strength, and percentage of elongation. Thus, no further material testing was carried out on the steelpipe. The experiments only covered a simple tensile test to obtain the material properties for the glass epoxy and a series of burst tests to measure the performance of the thermosetting liner.

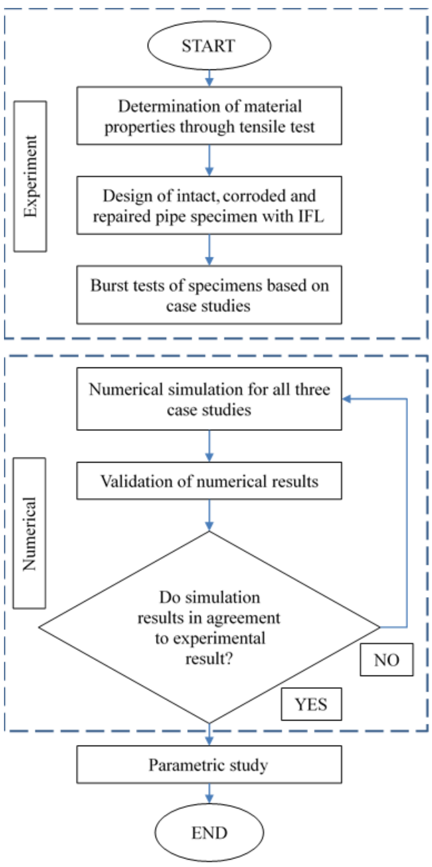

Fig. 5 Flow of research on determining the performance of thermosetting liners in burst capacity

Table 2 Thickness of tensile specimens with respect to the number of layers

Specimen	1 layer (mm)	2 layers (mm)	3 layers (mm)	4 layers (mm)	5 layers (mm)
1	0.466	0.792	1.386	1.688	1.88
2	0.462	0.82	1.25	1.516	1.91
3	0.456	0.812	1.302	1.548	1.888
4	0.426	0.824	1.324	1.51	1.932
5	0.442	0.81	1.35	1.662	1.916
Average	0.4504	0.8116	1.3224	1.5848	1.9052

3.1.1 Tensile test

The tensile test was conducted for glass epoxy in terms of the number of layers from 1 to 5 layers. The fiber directions were in the orientations of 0° and 90° direction. The tensile test was conducted following the standard of ASTM D638 using dog bone shape specimens as shown in Fig. 6. The setup of the experiment is shown in Fig. 7. Five case studies were conducted with respect to the number of layers. For each case study, the tensile test was repeated five times. Herein, the thickness of the specimen corresponded to the number of layers. The average thickness of the specimens for each case study are shown in Table 2. The tensile test was expected to yield results in terms of the Young's Modulus and ultimate tensile strength.

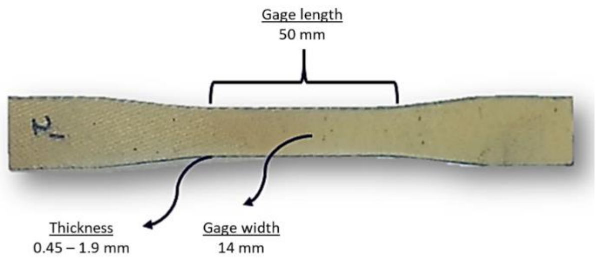

Fig. 6 Shape and dimension of tensile test specimen

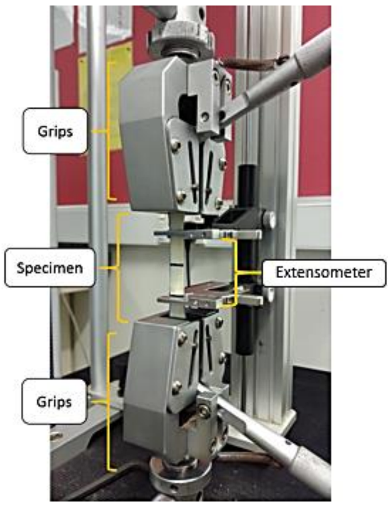

Fig. 7 Tensile test setup using Universal Testing Machine

3.1.2 Burst test specimen design

The specimens used for the burst test were API 5L X42 steel pipes with diameter of 4 in. and length of 1 ft. Four case studies were conducted for the burst test, namely (i) intact pipe, (ii) pipe with corrosion defect, (iii) pipe under corrosion but repaired with thermosetting liner, and (iv) leaked pipe repaired with thermosetting liner. The aim was to measure the performance of the thermosetting liner by determining the increase of burst capacity of a pipe with corrosion defect after being repaired with a thermosetting liner. The specimen design of an intact pipe is shown in Fig. 8.

The specimen was fabricated with threading at both ends of the pipe in order to attach the end caps and seal the specimen. The specimen has a total length of 300 mm, thickness of 3 mm and an outer diameter of 108 mm. The specimen design of the intact pipe became the control specimen in other case studies. The pipe with corrosion defect was fabricated with a single defect on the inner surface of the pipe as shown in Fig. 9. The dimensions of the defect are shown in Fig. 10.

The shape of the defect was based on ASME B31G in the form of an elliptical defect. The dimensions were determined based on past literatures. The depth of defect was assumed to be acceptable between 12.5% to 80% of wall thickness as the corrosion assessment equation only applies for values within that given range. The length was taken such that it is more than 3t to represent a general corrosion rather than pitting type.

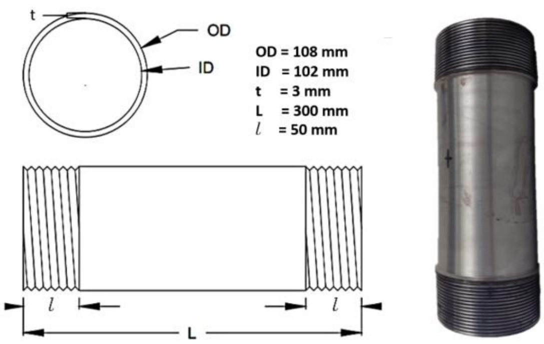

Fig. 8 Intact pipe design

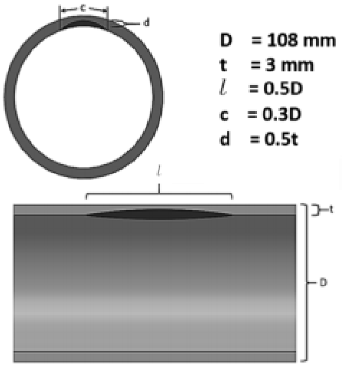

Fig. 9 Pipe sample with single corrosion defect

Width has little effect on the failure pressure (Belachew *et al.* 2011) and thus was not considered. The final dimensions of the defect with depth of 0.5t, length of 0.5D and width of 0.3D, were adopted from Netto *et al*. (2005) as they were within the acceptable range and were proven to yield reliable results at the end.

The third case study utilized the same pipe with corrosion but installed with a thermosetting liner as shown in Fig. 11. The glass epoxy prepregs was wrapped inside the inner surface of the pipe in three layers, an equivalent thickness of 0.84 mm and cured in an oven at temperature of 100ºC for 24 hours.

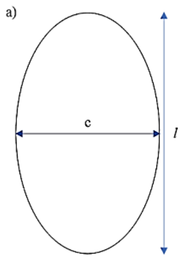

(a) Plan view

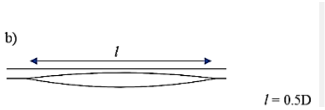

(b) Side view

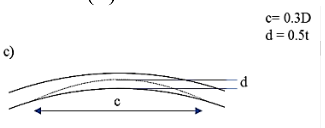

(c) Front view

Fig. 10 Dimensions of single corrosion

Fig. 11 Thermosetting liner installed inside a pipe specimen with corrosion

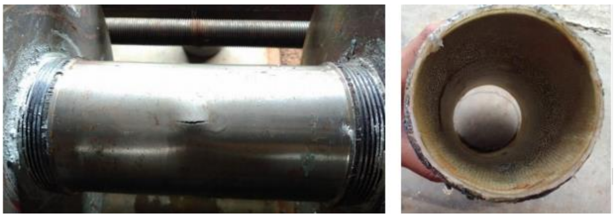

Fig. 12 Thermosetting liner placed in a leaked pipe

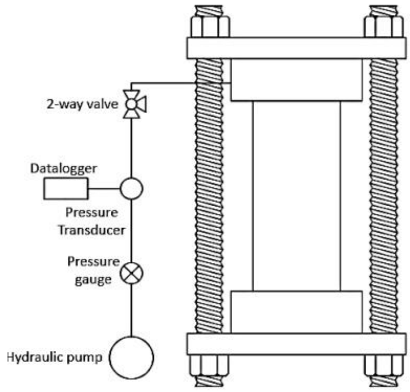

Fig. 13 Schematic diagram for burst test setup

(a) Hydraulic pump

(b) Pressure transducer

(c) Datalogger

(d) Hydraulic lines

Fig. 14 Individual component for burst test

The fourth case study involved a pipe with corrosion defect that was already burst, thus representing a leaked pipe as shown in Fig. 12.

3.1.3 Burst test setup

The test setup was largely referred to the works by Netto *et al.* (2005) with reference to Belachew et al. (2016) and Kim *et al*. (2002). The components of the setup consisted of a hydraulic pump, pressure gauge, pressure transducer, datalogger, burst rig, and hydraulic hoses to connect all components. The burst test was conducted by injecting water into the pipe specimen to induce internal pressure via the hydraulic lines and hydraulic pump.

A two-way valve was installed between the burst rig and pressure transducer for safety purposes. Since the water was pumped manually, the rate of pressure increment varied with time, but it could safely be said that based on the recorded data, the average pressure increment was only 2 bar/s. The pressure was monitored using the pressure gauge and pressure transducer which transferred to the data datalogger for recording. The schematic of the setup is depicted in Fig. 13, while the individual component is shown in Fig. 14.

The burst rig was custom made and comprised several parts required to be assembled for final finishing. The first step was connecting the pipe specimen to the end caps which were then clamped in between steel plates connected with twelve steel rods. The function of the end cap was to seal the open ends of the pipe specimen, while the end plates and steel rods were installed to resist tension forces produced by the internal pressure acting on the inner surface of the end cap. After completing the assembly, the burst rig was positioned in a horizontal manner with the help of a steel frame to avoid movement during testing. As such, the loads applied on the pipe specimen were limited to only radial internal pressure. The overall setup of the burst rig with the complete dimension is illustrated in Fig. 15, while the complete assembly is shown in Fig. 16.

3.2 Numerical simulation

The objective of the numerical simulation was to optimize the design of the thermosetting liner after validating results from the numerical model with the experiments. The flows of carrying out the simulation are shown in Fig. 17.

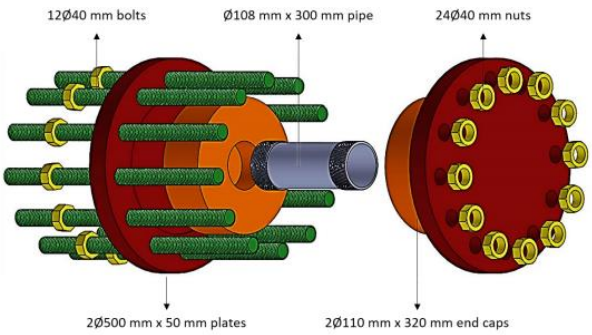

Fig. 15 Burst rig parts and dimensions

Fig. 16 Completed burst rig assembly

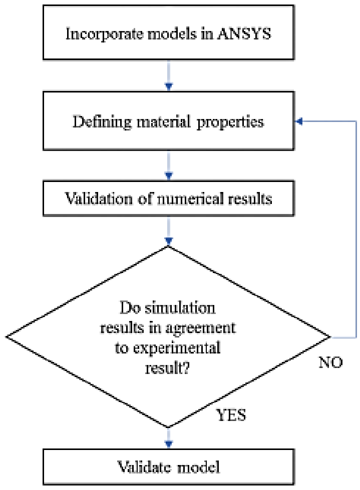

Fig. 17 Flow of numerical analysis

3.2.1 Material properties

The material properties for the API 5L X42 steel was defined using a constitutive equation, the Ramberg-Osgood equation adopted from Bedairi *et al.* (2012) and Andrade *et al.* (2006) as given in Eq. (1).

$$\varepsilon = \frac{\sigma}{E} + \left(\frac{\sigma}{\sigma_{YS}}\right)^{n-1}\left(\frac{\sigma}{E}\right) \tag{1}$$

Where,
Material constant, $\alpha = 1.75$
Material constant, $n = 9.35$
Yield strength, $\sigma_{YS} = 380$ MPa
Young's modulus, $E = 210$ GPa

The material properties for the glass epoxy prepreg was based on the simple tensile test conducted beforehand. However, the Young's Modulus obtained from the test was only applicable in the direction of the fiber reinforcement which is in the *x*-axis and *z*-axis. Therefore, the Young's Modulus in the transverse direction was calculated using Eq. (2) outlined by Kaw (1997). The equation is part of the general rule of mixture equations which is used to calculate the mechanical properties of a lamina. Although the equation is strictly for unidirectional lamina, it serves as a good estimation of the material's transverse Young's Modulus.

Table 3 Material properties defined for a three-layer glass epoxy prepreg

Material Properties		Value
Density (kg/m^3)		1302.8
Tensile Strength (MPa)		264
Young`s Modulus (GPa)	x-axis	8.5
	y-axis	8.5
	z-axis	12.11

$$\frac{1}{E} = \frac{V_f}{E_f} + \frac{V_m}{E_m} \tag{2}$$

Where:
Transverse modulus = E
Fiber volume fraction, $V_f = 0.7$
Matrix volume fraction, $V_m = 0.3$
Fiber Young's modulus, $E_f = 72$ GPa (Carpenter 2016)
Matrix Young's modulus, $E_m = 2.8$ GPa

The density was calculated using Eq. (3) outlined by Kaw (1997). The overall material properties of the glass epoxy prepreg used in the simulation are tabulated in Table 3. It should be noted that although the properties for the API 5L X42 steel was defined as nonlinear, the properties for the glass prepreg was defined as linear due to the brittle nature of the composite.

$$\rho_c = \rho_f V_f + \rho_m V_m \tag{3}$$

Where:
Density of composite = ρ_c
Fiber density, $\rho_f = 2600$ kg/m^3
Matrix density, $\rho_m = 1325.9$ kg/m^3
Fiber volume fraction, $V_f = 0.7$
Matrix volume fraction, $V_m = 0.3$

3.2.2 Meshing

The model was meshed using hexahedral solid elements due to the efficiency of the elements compared to tetrahedral elements (Owaisi *et al*. 2016) although both elements yield accurate results given that the mesh is sufficiently refined (Wang *et al.* 2004). Past literatures showed that at least three elements were needed through the thickness of the pipe to simulate an accurate deformation (Cronin 2000, Li 2016). Herein, all pipe models utilized gradually refined triangular mesh as shown in Fig. 18. These numbers were then changed accordingly based on a mesh sensitivity analysis where further addition of elements should yield less than 5% difference in result.

3.2.3 Boundary conditions

The boundary conditions were applied such that they resembled a clamped condition similar to those in experiments. The cross-section area was restricted in the x-axis while the end faces were restricted in the z-axis. A fixed point was applied at the edge of the model to establish a reference point for the model as shown in Fig. 19.

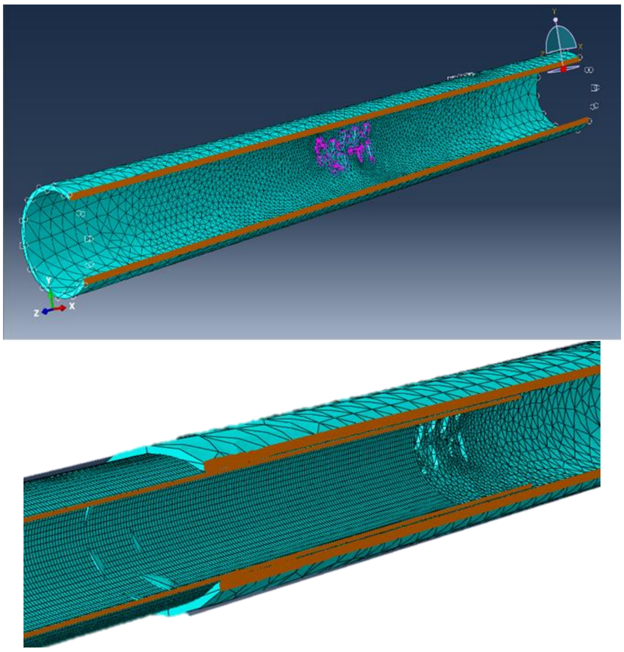

Fig. 18 Gradually refined triangular mesh model for pipe specimens in numerical model

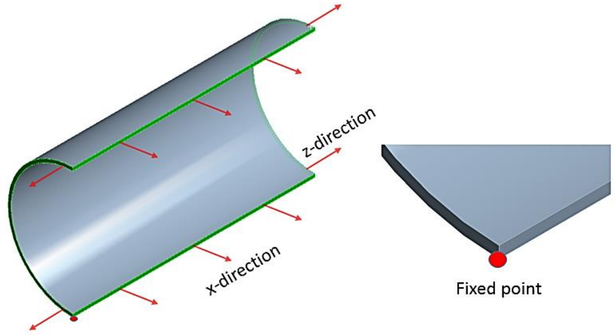

Fig. 19 Boundary conditions for numerical model

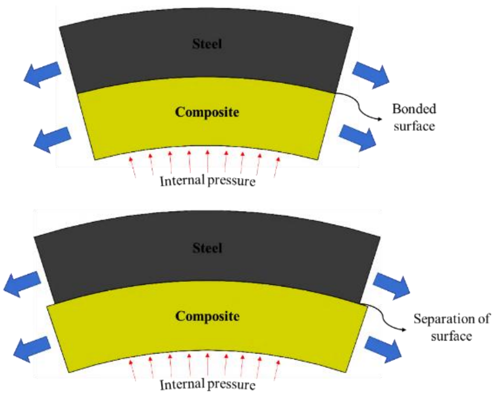

Fig. 20 Separation of surface between steel and composite due to deformation

The boundary conditions introduced were similar to those introduced in past literatures for symmetrical models and has proven to yield reliable results (Netto *et al.* 2005, Kim *et al.* 2002, Abdalla Filho 2014, Abdalla Filho 2010, Silva *et al*. 2007).

In the third case study, the contact between the outer surface of the thermosetting liner and the inner surface of the steel pipe was assumed to be bonded. The assumption was based on the failure mode reported by Farhidzadeh *et al.* (2014), where delamination was reported due to the different rates of deformation of the composite material and steel, as shown in Fig. 20. Even so, for any slippage to occur, it must overcome the frictional force which rises with normal force. Therefore, it is safe to assume that the contact between the composite and steel pipe as bonded.

3.2.4 Loadings

The loading applied in the simulation was pressure directed radially towards the inner surface of the pipe. The pressure was a static load as a preliminary simulation conducted using a time dependent loading with a rate of 0.2 MPa per second resulted in no difference to the final results.

3.2.5 Solutions

The results captured were in the form of failure pressure of the pipe. The failure criteria could either be stress-based or strain-based although the latter has been refuted by Chouchaoui and Pick (1996). Therefore, failure pressure was assumed when the von Mises stress was equal to the ultimate tensile strength at any points in the pipe, although it was expected to occur through the thickness of the pipe under the area of defect as mentioned in past literatures (Kim *et al.* 2002, Chen *et al.* 2015, Xu and Cheng 2012, Choi *et al*. 2003). The solutions obtained were then compared with experimental results for validation purposes.

3.3 Parametric study

The parametric study was conducted using the validated model of the pipe under corrosion defect and repaired with thermosetting liner. Note that the thickness of the thermosetting liner was defined in terms of the number of layers of glass epoxy, thus the total thickness of the thermosetting liner was determined from the cumulative thickness of the layers. In this paper, the parametric study was conducted for five layers with thickness tabulated in Table 4. In addition to the number of layers, the corrosion depth was also varied at 20%, 50%, and 80% corrosion depth. The boundary conditions, meshing, applied loadings, and material properties were similar to those outlined in the previous sections.

Table 4 Number of layers and corresponding thickness

Case	Number of Layers	Thickness (mm)
1	1	0.45
2	2	0.81
3	3	1.32
4	4	1.58
5	5	1.91

4. Results and discussion

4.1 Tensile test

The results obtained from the tensile tests are tabulated in Table 5. Note that the results shown in the last column of the table are the average results from the five specimens for each case study.

The average Young's Modulus obtained was 8.5 GPa, while the ultimate tensile strength was 167 MPa. These values were later incorporated into the material properties for the numerical analysis.

4.2 Burst test

The results of the burst test for each case study are tabulated in Table 6. The graphs of pressure with respect to time captured from the datalogger for each case study are shown in Figs. 21 to 24. Note that these graphs represented the increment of internal pressure induced to the inner surface of the pipe, through the manual pumping of the hydraulic pump system in the burst test set up. Since the pumping was made manual, the internal pressure imposed inside the pipe was increased gradually until it exploded (burst) at one point during the experiments, for which pressure dropped instantly after this point.

The initial slow rise of pressure, as shown in Figs. 21 to 24, was caused by the compressibility of water. As the water became completely compressed, the pressure started to rise linearly. At the point of burst failure, pressure started to drop completely, as shown in the figures.

Although the experiment setup was similar to that by Netto *et al.* (2005), comparison was made to the results obtained in ensuring better confidence in the data. Therefore, the results of the experiment were compared with current assessment methods to confirm the reliability of the method. The burst pressure of the intact pipe was compared with the Barlow formula, while the corroded pipe was compared with current assessment methods of corroded pipes, namely, ASME B31G, Modified ASME B31G, and DNV-RP-F101. The comparisons are shown in Tables 7 and 8. Note that no comparison was made for pipe with corrosion defect and repaired with the thermosetting liner due to the unavailability of reported resources similar to that of the experiments conducted.

The comparisons showed that for both intact pipe and those with corrosion, the differences captured were below 10%. Thus, it could be safely concluded that the experiments were validated. On another note, it could be seen that the assessment method for the corroded pipe, DNV-RP-F101, was conservative as compared to both the ASME B31G and Modified ASME B31G for its lowest results computed. This, however, was expected since DNV-RP-F101 assumes rectangular defects rather than circular which was applied in the experiment and allowing more metal loss.

4.2.1 Observations

The failure modes for the first three case studies are shown in Fig. 25. All specimens experienced ductile failure.

Table 5 Average Young's modulus and tensile strength of glass epoxy

Specimen	1	2	3	4	5	Average
Tensile Strength (MPa)	182.96	163.68	158.44	164.74	150.76	167.435
Young`s Modulus (MPa)	7856	51517	8512	9093	8688	8537

It was observed for the fourth case study that leakage occurred at approximately 14 MPa before ultimately failing at 17 MPa. The leakage as well as the failure during the test is shown in Fig. 26.

4.2.2 Discussion

The results of the burst test could be compared with other similar studies which are in the form of an external composite sleeve. Mazurkiewicz *et al.* (2017) reported that the improvement between intact pipe and those repaired with a glass epoxy sleeve was found to be 43.7%, which was almost double the amount observed herein. Duell *et al.* (2008) have also reported similar statement where the difference between corroded pipe and those repaired with a carbon epoxy sleeve produced an increase in strength by 67%.

The reason for the large gap of improvement between this research and other studies was probably due to the thickness of the material as well as the type of material used. Mazurkiewicz *et al.* (2017) applied a glass epoxy sleeve with a thickness of 2.5 mm, while the present research applied a thickness of 1.32 mm. On the other hand, Duell *et al.* (2008) used carbon fibers which are slightly superior in terms of tensile strength than glass fibers. Furthermore, the thickness of the sleeve applied was six layers, accumulating to a total thickness of 3.1 mm. Therefore, if the thickness of the thermosetting liner was doubled, the improvement in burst pressure could be comparable to that reported by Mazurkiewicz *et al.* (2017) and Duell *et al.* (2008).

Table 6 Results of burst test for each case study

Case study	Without liner (MPa)	With liner (MPa)
Intact pipe	25.1	-
Pipe with corrosion defect	17.09	23.02
Pipe with leakage	0	17

*Note: 1 MPa = 10 bar

Table 7 Comparison of experimental result from intact pipe with empirical equation

Assessment method	Burst pressure (MPa)	Difference (%)
Experiment	25.1	-
Barlow Formula	26.67	6.26

Table 8 Comparison of experimental result from pipe with corrosion defect with corrosion assessment methods

Assessment method	Burst pressure (MPa)	Difference (%)
Experiment	17.09	-
ASME B31G	17.68	3.45
Modified ASME B31G	16.26	4.86
DNV-RP-F101	15.43	9.71

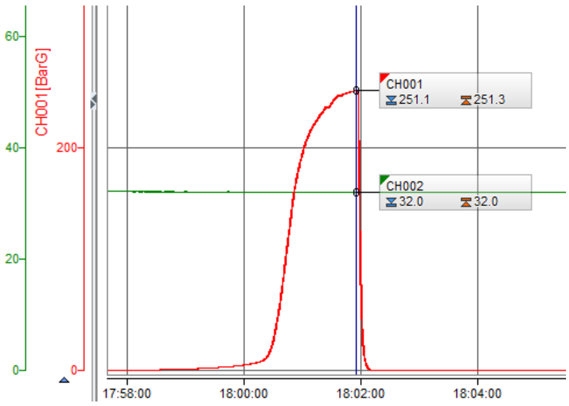

Fig. 21 Graph of pressure against time as captured by the datalogger for intact pipe

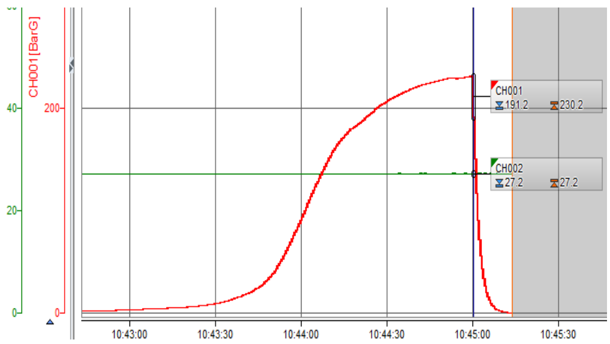

Fig. 22 Graph of pressure against time for as captured by the datalogger for pipe with corrosion defect

In addition to that, the fact that leakage was observed in the steel pipe for the pipe with leakage and repaired with thermosetting liner implied that water penetration has begun at around 14 MPa.

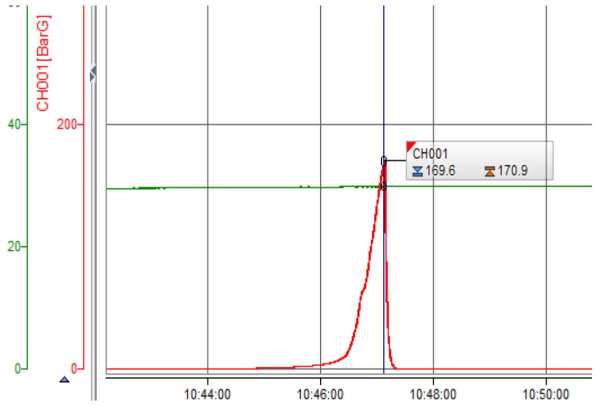

Fig. 23 Graph of pressure against time as captured by the datalogger for pipe with corrosion defect and repaired with thermosetting liner

Fig. 24 Graph of pressure against time as captured by the datalogger for pipe with leakage and repaired with thermosetting liner

The cause of penetration was due to cracks appearing on the thermosetting liner as glass epoxy has lower failure strain than steel. The failure strain of steel was calculated to be at 0.04 from the Ramberg Osgood equation, while the failure strain of glass epoxy was measured to be 0.02 from the tensile test.
Therefore, it can be concluded that the thermosetting liner would fail first before the steel pipe. This was also observed from a similar study by Mazurkiewicz *et al*. (2017) although the composite layer was applied on the outer layer of the pipe as a sleeve as shown in Fig. 27. Based on experiment and numerical simulation by Mazurkiewicz *et al.* (2017), it was shown that the glass epoxy sleeve failed first before the steel pipe, as shown in Fig. 27.

4.2.2 Discussion

The results of the burst test could be compared with other similar studies which are in the form of an external composite sleeve. Mazurkiewicz *et al.* (2017) reported that the improvement between intact pipe and those repaired with a glass epoxy sleeve was found to be 43.7%, which was almost double the amount observed herein. Duell, Wilson and Kessler (2008) have also reported similar statement where the difference between corroded pipe and those repaired with a carbon epoxy sleeve produced an increase in strength by 67%.

The reason for the large gap of improvement between this research and other studies was probably due to the thickness of the material as well as the type of material used. Mazurkiewicz *et al*. (2017) applied a glass epoxy sleeve with a thickness of 2.5 mm, while the present research applied a thickness of 1.32 mm. On the other hand, Duell *et al*. (2008) used carbon fibers which are slightly superior in terms of tensile strength than glass fibers. Furthermore, the thickness of the sleeve applied was six layers, accumulating to a total thickness of 3.1 mm. Therefore, if the thickness of the thermosetting liner was doubled, the improvement in burst pressure could be comparable to that reported by Mazurkiewicz *et al*. (2017) and Duell *et al*. (2008).

In addition to that, the fact that leakage was observed in the steel pipe for the pipe with leakage and repaired with thermosetting liner implied that water penetration has begun at around 14 MPa. The cause of penetration was due to cracks appearing on the thermosetting liner as glass epoxy has lower failure strain than steel. The failure strain of steel was calculated to be at 0.04 from the Ramberg Osgood equation, while the failure strain of glass epoxy was measured to be 0.02 from the tensile test.

Therefore, it can be concluded that the thermosetting liner would fail first before the steel pipe. This was also observed from a similar study by Mazurkiewicz *et al*. (2017) although the composite layer was applied on the outer layer of the pipe as a sleeve as shown in Fig. 27. Based on experiment and numerical simulation by Mazurkiewicz *et al.* (2017), it was shown that the glass epoxy sleeve failed first before the steel pipe, as shown in Fig. 27.

4.3 Numerical analysis

The results of the numerical analysis of each case study was validated with the experiments. The numerical result was considered validated when the percentage difference was less than 10%. However, the use of Ramberg-Osgood model was first validated with past literatures in order to determine that the model was applied correctly in the analysis as shown in Table 9. The results obtained for each reference was within 10% difference, thus validating the methods accordingly.

4.3.1 Intact pipe

The results of the mesh convergence study are shown in Table 10. The final results of the simulation were compared with the experiment result as well as the Barlow formula for validation purposes as shown in Table 11.

4.3.2 Pipe with corrosion defect

A mesh convergence study was conducted to ensure accurate result of the simulation as shown in Table 12. The final results of the simulation were then compared with the experiment result and other assessment methods for validation purposes as shown in Table 13.

(a) Intact pipe (b) Pipe with corrosion defect (c) Pipe with corrosion defect and repaired wi th thermosetting liner

Fig. 25 Failure modes of specimens for different pipes

(a) Leakage at 14 MPa (b) Failure at 17 MPa

Fig. 26 Leakage and failure during the test

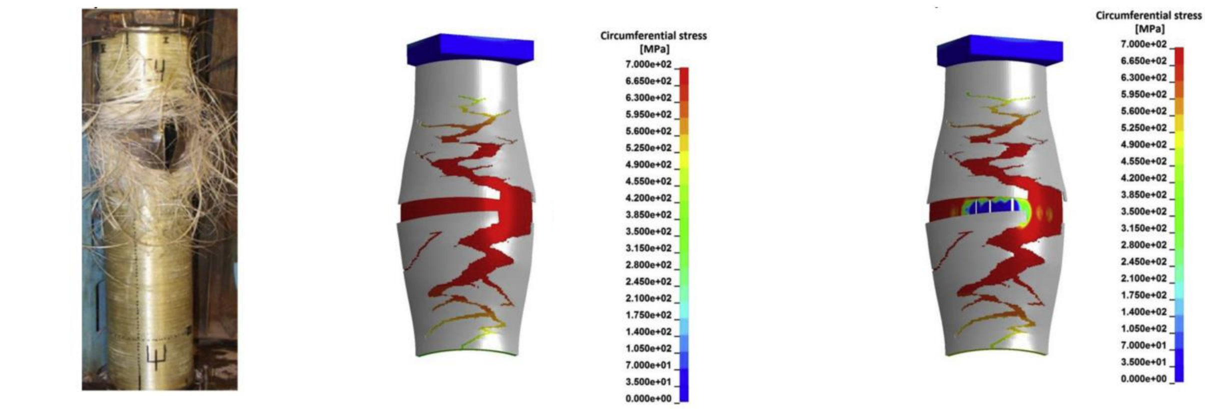

(a) Pipe after experiment test (b) Circumferential stresses from numerical analysis before failure (c) Circumferential stresses from numerical analysis after failure

Fig. 27 Pipe failures reported by Mazurkiewicz *et al.* (2017)

Table 9 Validation of method with past literatures

Reference	Pipe defects details	Published FEA Failure Pressure (MPa)	FEA Failure pressure in this work (MPa)	Difference (%)
Netto *et al*. (2005)	AISI 1020 OD: 41.94 mm t: 2.73 mm Circular defect d: 1.58 mm l: 42 mm c: 13 mm	38.92	35.1	9.8%
Bedairi *et al.* (2012)	X60 OD: 508 mm t: 5.7 mm Rectangular defect d: 45% l: 200 mm w: 30 mm	9.47	9.42	0.5%

4.3.3 Corroded pipe repaired with thermosetting liner

In order to determine the reliability of the method of analysis, especially regarding the bonded contact between the thermosetting liner and the inner surface of the host pipe, the method of analysis was first validated by repeating the simulation conducted by Mazurkiewicz *et al.* (2017). The study conducted by Mazurkiewicz *et al.* (2017) involved a glass epoxy sleeve wrapped around a Steel 20 pipe. The study consisted of four cases, but only one case was chosen for validation due to simplicity of the model i.e., an intact pipe installed with a glass epoxy sleeve as shown in Fig. 28. The material properties used by Mazurkiewicz *et al.* (2017) for Steel 20 and glass epoxy are shown in Tables 14 to 15. Failure was assumed to take place when the stress experienced by steel reached the maximum tensile strength, which was around 590 MPa. The contact was not stated by Mazurkiewicz *et al.* (2017) and thus is assumed to be bonded in the simulation. Table 16 shows the comparison between the result of the simulation conducted by Mazurkiewicz *et al.* (2017) and the present work.

Table 10 Mesh convergence study

Equivalent Stress (MPa)	Change (%)	Nodes	Elements
481.42	-	37791	6700
481.8	0.0788	210922	114618

Table 11 Validation of results for intact pipe

Assessment method	Burst pressure (MPa)	Difference (%)
Experiment	25.1	0
Barlow Formula	26.67	6.26
Numerical Analysis	26.5	5.58

Table 12 Mesh convergence for corroded pipe

Equivalent Stress (MPa)	Change (%)	Nodes	Elements
484.88	-	123775	24351
485.49	0.126	157286	32548

Table 13 Validation of results for pipe with corrosion defect

Assessment method	Burst pressure (MPa)	Difference (%)
Experiment	17.09	-
ASME B31G	17.68	3.45
Modified ASME B31G	16.26	4.86
DNV-RP-F101	15.43	9.71
Numerical Analysis	16.5	3.45

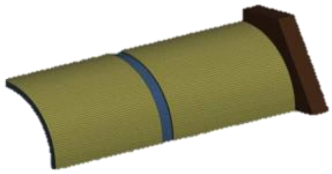

Fig. 28 Model of intact pipe installed with glass epoxy sleeve (Mazurkiewicz *et al.* 2017)

The result showed a difference of less than 10% between the FEA and experimental results between the present work and Mazurkiewicz *et al.* (2017). Therefore, the method of analysis including the type of contact defined was validated. The material property used for the glass epoxy prepreg was based on earlier tensile test, as tabulated in Table 17. The results of the numerical simulation for pipe with corrosion defect and repaired with thermosetting liner is tabulated in Table 18.

Results from the simulation showed a difference of less than 10% when compared with the experiments. Thus, the numerical model used for pipe with corrosion defect and repaired with thermosetting liner was considered validated.

4.3.4 Pipe with leakage repaired with thermosetting liner

The experimental results for the pipe with leakage and repaired with thermosetting liner showed that the liner ultimately failed at 17 MPa, while a complete leak was observed at 14 MPa. This suggests that failure has begun to occur in between the range of 14 to 17 MPa. Therefore, in the numerical simulation, 17 MPa was taken as the burst pressure of the thermosetting liner and failure was assumed when the von mises stress of the thermosetting liner was equal to the ultimate tensile strength of the glass epoxy i.e., 170 MPa as measured in the tensile tests. Based on these parameters, a mesh convergence study was conducted as shown in Table 19. The results of the simulation were then compared with experimental results as shown in Table 20.
The results showed a 12.94% difference between the simulation and experiment. This, however, was taken as the highest difference as the failure pressure could possibly occur as low as 14 MPa. Furthermore, the result difference could be attributed to other factors such as quality of machining or non-uniform thickness as reported by Mazurkiewicz *et al.* (2017). Thus, it was safe to assume that the numerical model for the pipe with corrosion defects and repaired with the thermosetting liner has been validated.

4.4 Parametric study

The parametric study was conducted based on the validation of the third case study involving pipe with corrosion defect and repaired with thermosetting liner.

Table 14 Material properties of Steel 20

Density (kg/mm^3)	Young's modulus GPa)	Poisson ratio	Yield strength (MPa)	Failure strain
7.830×10^{-9}	200	0.3	305	0.33

Table 15 Material properties of glass epoxy (Mazurkiewicz *et al.* 2017)

Material Property	Property Value
Young's modulus in *x-direction*, E_x (GPa)	48.47
Young's modulus in *y-direction*, E_y (GPa)	6.77
Young's modulus in *z-direction*, E_z (GPa)	6.77
Poisson ratio in *xy-direction*, υ_{xy}	0.099
Poisson ratio in *zx-direction*, υ_{zx}	0.099
Poisson ratio in *xz-direction*, υ_{xz}	0.4
Shear modulus in *xy-direction*, G_{xy} (MPa)	3.2
Shear modulus in *zx-direction*, G_{zx} (MPa)	3.2
Shear modulus in *xz-direction*, G_{xz} (MPa)	1.67

Table 16 Validation of method with past literatures

Reference	Published FEA Failure Pressure (MPa)	FEA Failure pressure in this work (MPa)	Difference (%)
Mazurkiewicz *et al.* (2017)	38.50	37.70	2.07

Table 17 Material properties of glass epoxy

Material Property	Property Value
Young's modulus in *x-direction*, E_x (GPa)	8.5
Young's modulus in *y-direction*, E_y (GPa)	8.5
Young's modulus in *z-direction*, E_z (GPa)	12.11
Poisson ratio in *xy-direction*, υ_{xy}	0.099
Poisson ratio in *zx-direction*, υ_{zx}	0.099
Poisson ratio in *xz-direction*, υ_{xz}	0.4
Shear modulus in *xy-direction*, G_{xy} (MPa)	3.2
Shear modulus in *zx-direction*, G_{zx} (MPa)	3.2

Table 18 Validation of result for pipe with corrosion defect and repaired with thermosetting liner

Assessment method	Burst pressure (MPa)	Difference (%)
Experiment	23.02	0
Numerical Analysis	20.9	9.13

Table 19 Mesh convergence for pipe with leakage and repaired with thermosetting liner

Elements	Nodes	Equivalent Stress (MPa)	Change (%)
11788	64970	178.05	0
24960	137004	172.70	3.004
26079	146079	172.74	0.0232

Table 20 Validation of result for pipe with leakage and repaired with thermosetting liner

Assessment method	Burst pressure (MPa)	Difference (%)
Experiment	17	0
Numerical Analysis	14.8	12.94

Table 21 Validation of pipe with corrosion defects at different corrosion depths

Corrosion depth	Numerical result (MPa)	Modified ASME B31G (MPa)	Difference (%)
20%	21.1	21.08	0.09
80%	10.4	10.46	0.57

Table 22 Simulation result for pipe with corrosion defect at 20% corrosion depth

No. of layer	Pressure (MPa)	Strength restoration	Strength increment (MPa)
0	21.1	-15.6% (3.9 MPa)	-
1	23.2	53.84%	2.1
2	24.7	92.3%	1.5
3	27.0	151.3%	2.3

Table 23 Simulation result for pipe with corrosion defect at 50% corrosion depth

No. of layer	Pressure (MPa)	Strength restoration	Strength increment (MPa)
0	17	-32% (8 MPa)	-
1	17.5	6.25%	0.5
2	19.0	25%	1.5
3	20.9	48.8%	1.9
4	21.9	61.25%	1.0
5	24.0	87.5%	2.1

Table 24 Simulation result for pipe with corrosion defect at 80% corrosion depth

No. of layer	Pressure (MPa)	Strength restoration	Strength increment (MPa)
0	10.4	-58% (14.6 MPa)	-
1	11.6	6.2%	1.2
2	12.1	11.03%	0.5
3	14.8	29.6%	2.7
4	16.1	38.6%	1.3
5	17.0	44.8%	0.9

The objective of the parametric study was to determine the minimum number of layers required to restore the original strength of the pipe with corrosion. This was executed by conducting simulations of a pipe with corrosion defect and repaired with thermosetting liner and varying the thickness of the thermosetting liner. The thickness depends on the corresponding number of layers. In this parametric study, the number of layers simulated were 1 to 5 layers.

In addition to that, the corrosion depth was also varied to see the effect of corrosion on the performance of the thermosetting liner. Three depths of corrosion were proposed which are 20, 50 and 80%. These values represent the minimum, mean, and maximum corrosion, respectively. The results of this parametric study were presented in the form of three case studies, where each case study represents a different depth of corrosion. For each depth of corrosion, five simulations were conducted with different number of layers from 1 to 5 layers.

However, to measure the strength increment and restoration, the results of the parametric study were compared with a pipe with corrosion defect without thermosetting liner. For the case of a corroded pipe with 50% depth of corrosion, note that the numerical model has been validated as explained in previous sections. However, the numerical model for a pipe with corrosion depths of 20 and 80% were yet to be validated. Thus, using the same material properties of API 5L X42 steel pipe in the previous sections, the numerical model for the pipe with corrosion was validated with corrosion assessment Modified ASME B31G as shown in Table 19. The results of the parametric study are shown in Tables 21 to 23.

The strength restoration was calculated based on the reduction of strength. Thus, for lower depths of corrosion, it was expected that the restorations of strength were very high. On the other hand, it could also be seen that, with each addition of layer, the burst capacity increased in between 0.5 to 2.7 MPa. The increment of strength was low because each addition of layer only added a thickness of roughly 0.5 mm.

From the results of the parametric study, the optimum thickness of the thermosetting liner could then be deduced with respect to the corrosion depth. By referring to the results obtained in Tables 22 to 24, discussion herein will be focusing on the closest values computed to achieve full restoration (i.e., 100%). For 20% of corrosion, 2 layers of thermosetting liner would give up to 92.3% of strength restoration, while for the 50% corrosion depth, the 5 layers was computed to provide 87.5%. The 80% corrosion depth when repaired with 5 layers of thermosetting liner provided strength restoration of 44.8% only. Thus, these values would provide some guidance on the performance of different layers of thermosetting liner towards strength restoration.

The results obtained in the parametric study only covered specific wall thickness and grade of steel pipe. Thus, it does not represent results for different grades of steel pipe with the same thickness and defect. Also, interested readers are advised to continue the assessment for the number of layers of thermosetting liner which are beyond the scope of the present work.

5. Conclusions

The experimental and numerical simulations conducted have proven that, where burst capacity is concern, thermosetting liners are capable of rehabilitating pipe with corrosion defects. In the burst test, it was shown that a 3 layer thermosetting liner is able to restore 23% burst capacity of the pipe with corrosion defects.

On the other hand, the numerical simulation has shown the optimum thickness of thermosetting liner required to restore the original strength of corroded pipes. For an API 5L X42 steel pipe with a wall thickness of 3 mm, having corrosion of 20, 50, and 80%, different values of strength restorations have been computed. For 20%, the closest value to full restoration was obtained as 92.3%, while for the 50 and 80%, further simulations are recommended on the number of layers of thermosetting liner which are beyond the scope of the present work.

However, further tests are required to fully qualify this repair method such as the installation and fabrication methods. Nevertheless, this research provides a starting point in qualifying the thermosetting liner as a rehabilitation method for corroded pipelines.

Acknowledgments

The authors gratefully acknowledged the support provided by Universiti Teknologi PETRONAS and Ministry of Higher Education (MOHE) of Malaysia for this work under Fundamental Research Grant Scheme (FRGS) 0153AB-L65.

References

4 Subsea. (2013), "Un-bonded flexible risers – Recent field experience and actions for increased robustness", for PSA - Norway, Stavange.

Abdalla Filho, J., Machado, R., Bertin, R. and Valentini, M. (2010), "Evaluation of residual strength of pipelines containing corrosion defects", *Proceedings of the 10th International Conference on Computational Structures Technology*.

Abdalla Filho, J., Machado, R., Bertin, R. and Valentini, M. (2014), "On the failure pressure of pipelines containing wall reduction and isolated pit corrosion defects", *Comput. Struct.*, **132**, 22-33. https://doi.org/10.1016/j.compstruc.2013.10.017.

Abel, T. (2015), "Laboratory tests of pipelines reinforced with close-fit Trolining liner", *Archiv. Civil Mech. Eng.*, **15**(2), 427-435. https://doi.org/10.1016/j.acme.2014.11.002.

Abel, T. (2015), "Changes in strength parameters of pipelines rehabilitated with close-fit trolining liners – Numerical analysis based on laboratory tests", *Archiv. Civil Mech. Eng.*, **16**(1), 30-40. https://doi.org/10.1016/j.acme.2015.09.002.

Al-Owaisi, S., Becker, A. and Sun, W. (2016), "Analysis of shape and location effects of closely spaced metal loss defects in pressurised pipes", *Eng. Fail. Anal.*, **68**, 172-186. https://doi.org/10.1016/j.engfailanal.2016.04.032.

Anderson, T. D., Kulkarni, M.G. and Macia, M. L. (2012), "Reinforced liners for long-distance pipeline rehabilitation", *Proceedings of the 22nd International Offshore and Polar Engineering Conference (ISOPE)*, 4, 395-400.

Barsoum, I., Dymock, J., Walters, R. and Seibi, A. (2016), "Finite element analysis of the installation process of a corrosion protective kevlar reinforced liner", *Abu Dhabi International Petroleum Exhibition & Conference*.

Bedairi, B., Cronin, D., Hosseini, A and Plumtree, A. (2012), "Failure prediction for crack-in-corrosion defects in natural gas transmission pipelines", *Int. J. Pressure Vessels Piping*, **96-97**, 90-99. https://doi.org/10.1016/j.ijpvp.2012.06.002.

Belachew, C.T., Ismail, M.C. and Karuppanan, S. (2011), "Burst strength analysis of corroded pipelines by finite element method", *J. Appl. Sci.*, **11**(10), 1845-1850. DOI: 10.3923/jas.2011.1845.1850.

Belachew, C.T., Mokhtar, C.I. and Karuppanan, S. (2016), "Strength assessment of a corroded pipeline through the burst test: case study", *J. Pipeline Syst. Eng. Practice*, **7**(3), 3-8. https://doi.org/10.1061/(ASCE)PS.1949-1204.0000232.

Carpenter, C. (2016), "Mechanical characterization and corrosion effects on glass reinforced vinyl ester liners used for oil and gas production", *Society of Petroleum Engineers (SPE) Annual Technical Conference and Exhibition*.

Chen, M. and Das, S. (2009), "Experimental Study on repair of corroded steel beam using CFRP." *Steel Compos. Struct*., **9**(2), 103-118. https://doi.org/10.12989/scs.2009.9.2.103.

Chen, Y., Zhang, H., Zhang, J., Liu, X., Li, X. and Zhou, J. (2015), "Failure assessment of X80 pipeline with interacting corrosion defects", *Eng. Fail. Anal.*, **47**, 67-76. https://doi.org/10.1016/j.engfailanal.2014.09.013.

Choi, J., Goo, B., Kim, J., Kim, Y. and Kim, W. (2003), "Development of limit load solutions for corroded gas pipelines", *Int. J. Press. Vessels Piping*, **80**(2), 121-128. https://doi.org/10.1016/S0308-0161(03)00005-X.

Chouchaoui, B. and Pick, R. (1996), "Behaviour of longitudinally aligned corrosion pits". *Int. J. Press. Vessels Piping*, **67**(1), 17-35. https://doi.org/10.1016/0308-0161(94)00057-3.

Cronin, D.S. (2000), "Assessment of corrosion defects in pipelines", PhD thesis, *University of Waterloo.*

De Andrade, E.Q., Benjamin, A.C., Machado, P.R., Pereira, L.C., Jacob, B.P., Carneiro, E.G. and Noronha, D.B. (2006), "Finite element modeling of the failure behavior of pipelines containing interacting corrosion defects", *Proceedings of the 25th International Conference on Offshore Mechanics and Arctic Engineering (OMAE)*.

Do, A.T., Bernard, G. and Hanonge, D. (2013), "Carbon fiber armors applied to presalt flexible pipe developments", *Offshore Technology Conference*, 6-9.

Duell, J., Wilson, J. and Kessler, M. (2008), "Analysis of a carbon composite overwrap pipeline repair system", *Int. J. Press. Vessels Piping*, **85**(11), 782-788. https://doi.org/10.1016/j.ijpvp.2008.08.001.

Farhidzadeh, A., Dehghan-Niri, E., Zhong, Z., Salamone, S., Aref, A. and Filiatrault, A. (2014), "Post-earthquake evaluation of pipelines rehabilitated with cured in place lining technology using acoustic emission", *Constr. Build. Mater.*, **54**, 326-338. https://doi.org/10.1016/j.conbuildmat.2013.12.048.

Frost, S., Savidis, Y., Illson, T.F., Ashworth, R., Heath, S., Cambers, J. and Boot, J.C. (2000), *COREL (Corrosion Resistant Liners) Joint Industry Project (JIP)*", NACE International.

Hancox, N. (1991), "Elevated temperature polymer composites", *Mater. Design*, **12**(6), 317-321.

Hopkins, P. (2005), "High design factor pipelines: integrity issues", 44.

Kaw, A. K. (1997), *Mechanics of Composite Materials*. Taylor & Francis.

Keykha, A.H. (2017), "CFRP strengthening of steel columns subjected to eccentric compression loading", *Steel Compos. Struct.*, **23**(1), 87-94. https://doi.org/10.12989/scs.2017.23.1.087.

Kim, W., Kim, Y., Kho, Y. and Choi, J. (2002), "Full scale burst test and finite element analysis on corroded gas pipeline", *Proceedings of the 4th International Pipeline Conference, Parts A and B*, 1501-1508.

Li, X., Bai, Y., Su, C. and Li, M. (2016), "Effect of interaction between corrosion defects on failure pressure of thin wall steel pipeline", *Int. J. Press. Vessels Piping*, 138, 8-18.

Mazurkiewicz, L., Tomaszewski, M., Malachowski, J., Sybilski, K., Chebakov, M., Witek, M. and Dmitrienko, R. (2017), "Experimental and numerical study of steel pipe with part-wall defect reinforced with fibre glass sleeve", *Int. J. Press. Vessels Piping*, **149**, 108-119. https://doi.org/10.1016/j.ijpvp.2016.12.008.

Mehdi, M.S. and Al-dossary, A.K. (2013), "Thermoplastic lined pipework for corrosive applications", *Corros*, (2197), 1-7.

Mohammadi, K. (2011), "Repair methods for damaged pipeline beyond diving depth" University of Stavanger.

Muren, J. (2007), "Flexible pipes failure modes, inspection, testing and monitoring", *PSA - Norway*, 30.

Netto, T., Ferraz, U. and Estefen, S. (2005), "The effect of corrosion defects on the burst pressure of pipelines", *J. Constr. Steel Res.*, **61**(8), 1185-1204. https://doi.org/10.1016/j.jcsr.2005.02.010.

Nienartowicz, B. (2012), "Rehabilitation of sewer channels, Investigations of load capacity of channels renovated with GRP liners", in *Underground infrastructure of urban areas 2* (pp. 185-194). Boca Raton, FL: CRC Press.

Nienartowicz, B. (2015), "Analysis of selected aspects of the operations of pipelines renewed with the relining method on the basis of laboratory testing results", in *Underground infrastructure of urban areas 3*. (Eds., Boca Raton: C. Madryas, B. Przbyla, and A. Szot), CRC Press.

Obrien, P., Meldrum, E., Overton, C., Picksley, J., Anderson, K., and MacLeod, I. (2011), "Outcomes from the SureFlex joint industry project - an international initiative on flexible pipe integrity assurance", *Offshore Technology Conference*.

Palmer, A.C. and King, R.A. (2004), *Subsea Pipeline Engineering*.

Popineau, D., Wiet, P. and Boulet d'Aurias, S. (2012), "Subsea pipeline repair by composite system", Society of Petroleum Engineers.

Setvati, M.R. and Mustaffa, Z. (2018), "Rehabilitation of notched circular hollow sectional steel beam using CFRP Patch", *Steel Compos. Struct.*, **26**(2), 151-161. https://doi.org/10.12989/scs.2018.26.2.151.

Silva, R., Guerreiro, J. and Loula, A. (2007), "A study of pipe interacting corrosion defects using the FEM and neural networks", *Adv. Eng. Softw.*, **38**(11-12), 868-875. https://doi.org/10.1016/j.advengsoft.2006.08.047.

Simonsen, A., Janssen, E. and Paton, C. (2012), "Inspection and monitoring techniques for un-bonded risers and pipelines", University of Stavanger.

Sulaiman, N.S. and Tan, H. (2014), "Third party damages of offshore pipeline 海底管道的第三方损伤", *J. Energy Challenges Mech*, **1**(1), 1-6.

Walters, R.A. (2015), "IFL™ - A novel approach to the rehabilitation of sub-sea hydrocarbon pipelines using high performance solef PVDF flexible kevlar reinforced liners", *Society of Petroleum Engineers (SPE)*.

Wang, E., Nelson, T. and Rauch, R. (2004), "Back to Elements - Tetrahedra vs. Hexahedra", *CAD-FEM GmbH, Munich, Ger*, 16.

Wright, J.R., Karim, K.A. and Kennedy, S. (2014), "A case study detailing the design, planning, installation and cost and environmental benefit analysis of a reinforced thermoplastic pipe pulled through the inside of an existing offshore steel flow line in the East Malaysia Samarang Field", *Offshore Technology Conference-Asia*.

Xu, L. and Cheng, Y. (2012), "Reliability and failure pressure prediction of various grades of pipeline steel in the presence of corrosion defects and pre-strain", *Int. J. Press. Vessels Piping*, **89**, 75-84. https://doi.org/10.1016/j.ijpvp.2011.09.008.

Yang, Y., *et al*. (2017), "Study of the design and mechanical performance of a GFRP-concrete composite deck" *Steel Compos. Struct.*, **24**(6), 679-688. https://doi.org/10.12989/scs.2017.24.6.679.

CC